



REGULAR ARTICLE

Mechanism of Heat Release from Nickel or another Metal Filled with Hydrogen

V. Krasnoholovets*

Institute of Physics, NAS of Ukraine, 03028 Kyiv, Ukraine

(Received 02 September 2025; revised manuscript received 14 December 2025; published online 19 December 2025)

It is shown that the appearance of gamma radiation in composite metals filled with hydrogen occurs as a result of momentum resonance between scattered hydrogen diffusing in a polaron mode and a vibrating atom of the crystal lattice. The reason for the generation of extra heat in metal nanocomposites and grains is due to the scattering of an oscillating atom of the crystal lattice by hydrogen atoms, as a result of which a hydrogen cluster is formed obtaining the kinetic energy from the atom. The surrounding thermostat quickly returns the atom to thermal equilibrium, and only after that the cluster gives the captured energy back to the lattice atom, which increases the atom's kinetic energy, i.e., leads to an increase in the heating of the sample, and the cluster itself again breaks up into free atoms. Then this procedure is repeated again and again. Thus, a new feature of nanocomposite materials has been found, namely the possibility of short-term energy storage.

Keywords: Heat, Hydrogen, Inertons, Mass defect, Nanoparticles

DOI: [10.21272/jnep.17\(6\).06009](https://doi.org/10.21272/jnep.17(6).06009)

PACS numbers: 05.70.Ln, 52.59. – f, 67.63.Gh,
78.57.Bf, 82.60.Qr

1. INTRODUCTION

The first report on excess heat evolution measured on nickel, gold, silver, and tin in aqueous K_2CO_3 , Na_2CO_3 , Na_2SO_4 , and Li_2SO_4 solutions under galvanostatic electrolysis conditions was presented by Ohmori and Enyo [1] in 1993. Further studies on the release of excess heat from a nickel rod sample and then a plate sample filled with hydrogen were presented by Focardi et al. [2-5]. The researchers reported that gamma radiation was detected with the peak centred at keV [4, 5]. They [3] investigated the surface of the nickel samples that generated heat and revealed that the elemental analyses were very different from the blank rod analysis, and the elements were very different from one region to the next along the sample; in particular, the concentrations of such elements as Cr, Mn, Fe, Si significantly increased, which pointed to the transmutation of Ni to these elements.

Later, following Rossi's [6] claim on a possible new kind of heating device, the researchers [7] designed a special type of reactor tube charged with a small amount of hydrogen loaded nickel powder plus some additives. The reaction was primarily initiated by heat from the resistor coils inside the reactor tube, and as a result the reactor produced abnormal heat, at least twice as much as the heat generated by the resistor. The effect of such macroscopic heating was further studied by several researchers (see, e.g. Refs. 8, 9). Nevertheless, some authors [10, 11] expressed their criticism regarding the

correctness of the estimate of the additional heat release. This is probably because the effect of additional heating was only evident at a primary heating temperature of roughly 1100 °C, but the critics argue that at such a temperature it is extremely difficult and doubtful to determine the release of extra heat.

Recent research conducted with Ni-nanocomposite samples filled with H or D gases [11-15] do not show radiative processes, i.e. no harmful X-ray, γ -ray and neutron radiation were measured. The authors [13-21] have studied energy generation using nanosized multilayer metal composites (Ni, Cu, W, Mn, Pd, Zr_2O , and others) with hydrogen gas. They observed heat bursts and excess energy generation in experiments conducted under vacuum conditions. In paper [14], a heat-sink energy per D(H)-desorption was around 50-80 eV, and the authors noted that was too large to be explained by H(D)-bonding energy to any metal. Takahashi et. al [18] reported about a very large specific reaction energy as per D-transferred, namely, from 100 eV/D to 500 eV/D, although a weak (0.1-0.2 n/J level) neutron emission was also measured correlating with the momentary thermal power burst. Iwamura et al. [20, 21] stated that in their nanosized samples each hydrogen atom produced extra heat at a value of 16 keV [20] and 10 keV [21]. Kitamura et al. [16] studied D-Pd-Ni, H-Pd-Ni, and H-Cu-Ni systems and found that excess heat reached 480 eV per one deuterium and the maximum phase-averaged excess heat energy exceeded 270 keV/D, while single-element nanoparticle samples

* Correspondence e-mail: krasnoh@iop.kiev.ua



produced no excess power. They reasonably note that any chemical reaction cannot produce such heat and pose that these values make it realistic to assume a nuclear origin of the excess heat. Mizuno and Rothwell [22] demonstrated a method of producing excess heat with nickel mesh coated with palladium, which was filled with deuterium.

It should be noted that at a microscopic level, hydrogen absorption by metal is a complex multi-step process that begins with the dissociation of the H_2/D_2 molecule on the metal surface. We will not be tied to experiments with specific parameters, but will consider the picture in general, that is, we will examine those situations in which the phenomena declared by successful experimenters can be explained.

In this work, the main features of the processes occurring in metal samples filled with hydrogen are analysed from a theoretical point of view, considering the submicroscopic concept that the author has been developing over the years. Namely, reasons will be considered that lead to the appearance of gamma radiations and will examine required conditions and criteria allowing the mechanism of extra heat generation.

2. SCATTERING OF A HYDROGEN POLARON BY A LATTICE ATOM

Thus, the researchers [4, 5] measured gamma radiation from hot samples of nickel. We [23] observed a similar situation, that is, the appearance of gamma quanta during the formation of plasma in the gap between two tungsten electrodes at a discharge and a low value of the pulling electric field, in the study of the formation of subhydrogen (see also Refs. 24, 25). The radiation mechanism was as follows.

A proton strikes an atom from a cathode. The cathode as a typical metal has the crystal structure. In the crystal, each atom oscillates near its equilibrium position and its velocity varies from v_{atom} to 0. Due to the interaction with space, this has the structure of the tessellattice [25], any particle moves, emitting inertons that are spatial excitations that carry mass properties of the particle i.e. fragments of the particle mass. Hence, at some point the particle must stop, but after that, the tessellattice returns inertons back to the particle. In this process, the particle's de Broglie wavelength λ_{dB} plays the role of half the spatial period. Along the entire path of the particle, in each odd λ_{dB} section, the particle emits inertons and hence finally must stop ($v = 0$), and then in each even section, the particle absorbs its inertons back and restores its velocity ($v = v_p$). The particle's de Broglie wavelength is $\lambda_{\text{dB}} = h/(mv_p)$ where m and v_p are the particle mass and speed, respectively. The amplitude of the particle's inerton cloud is equal to $\Lambda = \lambda_{\text{dB}}c/v_p$ where c the speed of light is.

Therefore, two colliding particles, a proton and a tungsten atom, pass through different phase states over time. Even if they have the same momentum, they can collide while being in different phase states. A similar situation happened in the experiments [2-5]. One of the options is illustrated in Fig. 1.

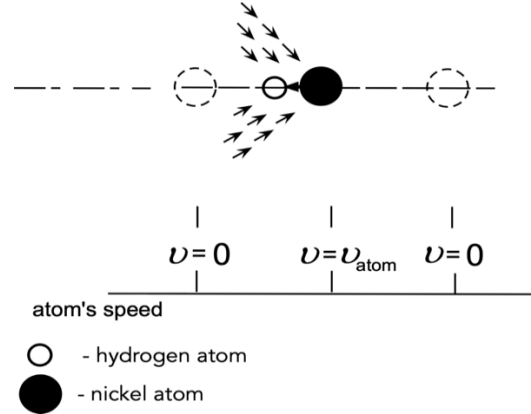


Fig. 1 – Momentum resonance collision of an incident hydrogen atom with an oscillating atom of the crystal lattice. The atom with the velocity v_{atom} passes its equilibrium position. The hydrogen atom collides with this atom in a phase when the hydrogen's velocity drops to almost zero. In this case the hydrogen's inerton cloud (thin arrows) passes to the atom

Fig. 1 shows how the hydrogen's inerton cloud joins the atom's inerton cloud. Of course, in the conditions of thermal diffusion, one cannot expect a complete transfer of the mass of the inerton cloud of the proton to the nickel atom. Most likely, only a small part of the proton inerton cloud is absorbed by the nickel atom. A mass δm emerges in the atom, which creates a mass excitation in it. The Hamiltonian of the atom can look as below

$$H = -\sum_i \frac{ze^2}{4\pi\epsilon_0 r_i} + \sum_j \frac{1}{2} \gamma r_j^2 \quad (1)$$

where the summation by i and j is carried out over all electrons of the system. Here the second term describes the resulting elastic energy in the atom due to the absorption of the mass defect δm . The atom has to straighten up and drop this excitation, which can be emitted into the lattice or the mass excitation can be removed via the radiation of a high-energy photon.

Since in the experiments [2-5] the photon radiation was regularly observed, it is reasonable to suggest that hydrogen atoms were tightly connected to the lattice phonons. Then an appropriate vibration mode brought hydrogens in the phase state shown in Fig. 1, to the atom whose vibration was coherent with the same mode.

The momentum of the oscillating atom Ni is

$$m_{\text{Ni}} v_{\text{Ni}} = m_{\text{Ni}} \sqrt{\frac{3k_B T}{m_{\text{Ni}}}} = \sqrt{3m_{\text{Ni}} k_B T}. \quad (2)$$

where the mass $m_{\text{Ni}} = 9.74627 \times 10^{-26}$ kg. In particular, at $T = 500$ K the momentum is equal to 4.49×10^{-23} kg·m·s⁻¹.

For the full momentum resonance, a hydrogen atom that collides with a nickel atom must also have the same value of the momentum. The rate of diffusion of hydrogen atoms is determined by the ambient temperature and also H must strongly be bound to the lattice vibrations. So, the momentum of a moving hydrogen H should look as below

$$m_H^* v_H = m_H^* \sqrt{\frac{3k_B T}{m_H^*}} = \sqrt{3m_H^* k_B T}. \quad (3)$$

where m_H^* is the effective mass of H , since hydrogen atoms are tightly bound to the lattice vibrations.

Comparing the two expressions, (2) and (3), it becomes obvious that the effective mass of a hydrogen atom should be equal to the mass of a nickel atom since only such equality ensures the momentum resonance. Of course, this is in an ideal case. Nevertheless, we need to understand how the hydrogen atom acquires its effective mass.

Fukai [26] inform us that compared too many other atoms in solids, hydrogen in metals exhibits rather fast diffusion. Hempelmann [27] reported an absolutely astonishing fact, namely, that the diffusion of hydrogen in metals occurs in accordance with the small polaron mechanism. The same also was proved in paper [28]. The researchers have used quasi-elastic neutron scattering, the unique feature of which is the simultaneous study of the diffusion process on atomistic scales of space and time. The author [27] cites experimental facts that confirm his correctness and indicates that the small polaron type of diffusion has been verified from low temperatures up to about 1000°C. He writes that the diffusion of hydrogen, deuterium and tritium in metals is located in the transition range between band-like transport (like electrons in metals) and classical jump processes that bring about the diffusion of heavy metal atoms. The small polaron theory provides an adequate description of the elementary diffusive steps of hydrogen, deuterium and tritium in the adiabatic and non-adiabatic temperature ranges. Hempelmann also emphasises that practically the whole spectrum of transport phenomena ranging from coherent tunnelling to almost classical jump diffusion can be studied in one system only. At very high temperatures, hydrogen undergoes gas-like diffusion in metals.

The authors [27–29] highlight that the diffusion of hydrogen in metals involves the basic ideas of Chudley and Elliott [30] on their diffusion jumping theory. Their diffusion theory allows one to estimate the duration of the jumping of hydrogen, which falls within an interval from pico- to nanoseconds. The small polaron mechanism involves collective vibrations of atoms (i.e., coherent optical phonon oscillations) to activate hydrogen jumps, so that the activation energy becomes a function of temperature T , namely [31]

$$E_a(T) = k_B T \sum_q |\Delta(q)|^2 \tanh[\hbar\Omega_q/(4k_B T)], \quad (4)$$

Here, $|\Delta(q)|^2 \gg 1$ is the coupling constant of hydrogen with nodes of the lattice, q is the wave number and Ω_q is the frequency of q -branch of phonons.

The latest measurements of the activation energy of hydrogen in nickel at room temperature give a value of 27.19 kJ·mol^{−1} [32], which is 4.515×10^{-20} J = 0.282 eV. Although for hydrogen atoms adsorbed on nickel films, the activation energies varies from 0.8 to 2.4 kcal·mol^{−1} [33], which is 5.608×10^{-21} to 1.666×10^{-20} J, or 0.035 to 0.104 eV, respectively (recall, a room temperature, $T = 300$ K, is about 0.026 eV). These measured values of hydrogen

activation energy are quite small and, consequently, the polaron mechanism can easily transfer hydrogen through the nickel sample studied. The researchers [34] investigated theoretically a distribution of hopping barriers for hydrogen in computer modelling, revealed that the barriers lie between 0.3 to 0.7 eV. They identified that the short- and long-range hydrogen arrangement and the hydrogen concentration influence the barrier.

Hempelmann [27] noted with elevating temperature a hydrogen atom alternates between a self-trapped state and an excited state that can also involves the continuous polaron movement. Diffusive behaviour is situated in the transition range between “jump diffusion” at room temperature and a gas-like hydrogen diffusion mechanism at very high temperatures.

These remarks allow us to compose a relation that accepts the estimation an effective mass m_H^* of the hydrogen atom that carried by the polaron mode. The relation should include the pre-exponential factor, i.e., an attempt frequency τ_0^{-1} of successful jumps (the dimension is s^{−1}), which thus is a time constant, but it does not require the activation energy given by an Arrhenius dependence since at a high temperature, hydrogen atoms behave as a gas, the diffusion of which practically does not show any barrier dependence. Then we can add a multiplier l_H that identifies the average distance between hydrogen atoms in the metal lattice, i.e., the jump length of a hydrogen atom. Hence the product $l_H \tau_0^{-1}$ represents the speed of a hydrogen atom that jumps from one position to another.

In such a way we may construct a relationship between the kinetic energy of the hydrogen atom and its activation energy presented in the theory of small polaron (since this is exactly the energy that the polaron has when rolling over a barrier):

$$\frac{1}{2} m_H^* (l_H \tau_0^{-1})^2 = k_B T \sum_q |\Delta(q)|^2 \tanh[\hbar\Omega_q/(4k_B T)] \quad (5)$$

From this equation we derive the expression for the effective mass of the hydrogen atom

$$m_H^* \approx \frac{1}{(l_H \tau_0^{-1})^2} \sum_q |\Delta(q)|^2 \hbar\Omega_q/4 \approx \frac{1}{(l_H \tau_0^{-1})^2} |\Delta(\bar{q})|^2 \hbar\Omega/4, \quad (6)$$

in which we take into account that in the small polaron theory at temperatures above 150 K the inequality $\hbar\Omega \ll 4k_B T$ holds.

The researchers [35] communicate that the H concentration in Ni is enhanced at high H₂ pressure, so that at 1000 K the H concentration increases from $n = 3.08 \times 10^{-4}$ H/Ni at a pressure of 1 bar to $n = 9.68 \times 10^{-3}$ H/Ni at a pressure of 10³ bar. Ni and Fe metals generally have a low critical hydrogen content, as low as parts per million in weight (wt. ppm, wppm, or μg/g), and even this small critical value of the hydrogen concentration results in a change of the ultimate tensile strength [34]. Consequently, nickel loses its strength when one nickel atom accounts for 1.7×10^4 or less hydrogen atoms, i.e. the critical concentration are $n_c = 5.88 \times 10^{-5}$ H/Ni. Therefore, for the stable existence of the small polaronic hydrogen state, the crystal lattice must

be regular, which is possible with the concentration of hydrogen $n < n_c$. Hence the average distance between hydrogen atoms in the metal lattice should be $l_H > (5.88 \times 10^{-5} n_{Ni})^{-3} \approx 5.74 \times 10^{-9}$ m where $n_{Ni} = 9 \cdot 10^{28} \text{ m}^{-3}$ is the concentration of nickel atoms.

So, in the expression for the effective mass (5) we can put the following values of the parameters: $l_H \approx 10^{-6}$ m, $\tau_0^{-1} \approx 10^8 \text{ s}^{-1}$, $\Omega \approx 10^{11} \text{ s}^{-1}$ and $|\Delta(\bar{q})|^2 \approx 588$. These parameter values lead us to an effective mass of hydrogen equal to the mass of a nickel atom, $m_H^* = m_{Ni} = 9.74627 \times 10^{-26}$ kg, which ensures the momentum resonance, (2) and (3). The value of the activation energy of the considered hydrogen polaron (4) is 0.0068 eV.

Despite the successfully selected parameters needed to derive the value of m_H^* , which satisfies strict total momentum resonance, we must take into account the remarks [27, 30] regarding the value of the hydrogen atom jump rate constant τ_0^{-1} : it lies within a pico- or nanosecond. Therefore, by imposing the inequality $5 \cdot 10^9 \text{ s}^{-1} < \tau_0^{-1} < 10^{11} \text{ s}^{-1}$, we obtain the limits of the corresponding values of the effective mass of a hydrogen atom, which is almost resonantly scattered by the lattice atom (nickel, palladium, etc.):

$$m_H^* \approx 10^{-31} \text{ to } 5 \cdot 10^{-30} \text{ kg.} \quad (7)$$

The same range of values corresponds to the mass defect δm that captures the nickel atom from the hydrogen atom, and then this absorbed (elastic) energy can either pass into the crystal lattice, or be released as an emitted gamma quantum in the appropriate range from several tens of keV to several MeV, which in fact was detected [4, 5].

3. GAMMA RADIATION

How gamma quanta are really generated? It is the matter of fact that gamma rays are created by nuclear decay, although Focardi et al. [4] and Campari et al. [5] emphasise that the appearance of gamma rays in nickel and other materials, which were simply filled with hydrogen, are unexpected and unexplainable within the frame of present physical theories. They also point out that the gamma spectra observed are different from those produced by neutrons impinging on the detectors.

According to the theory presented above, the hydrogen atom (Fig. 1) emits its inertons in the direction of the nearest atom of the metal lattice. The number N of emitted inertons can be estimated by dividing the hydrogen polaron's de Broglie wavelength λ_{dB} by the cell size (Planck's length $\ell_P \sim 10^{-35}$ m) of the tessellattice. The wavelength $\lambda_{dB} = h/(m_H^* v_H)$ can be estimated using expressions (3) and (7), which equals crude from 10^{-7} to 10^{-8} m. Therefore, $N = \lambda_{dB}/\ell_P \sim 10^{26}$ to 10^{27} inertons.

So, each inerton carries away from the hydrogen polaron an energy $\mu_i c^2$ where μ_i is the mass of the i th inerton and c is the speed of light, i.e. c is the speed of sound of the tessellattice that transfers its mass excitations (as well as photon excitations) [25]. Inertons emitted by a free moving

particle travel a distance equal to the amplitude of the inertons cloud $\Lambda = \lambda_{dB} c/v \approx 10^{-5} - 10^{-6}$ m where they stop and then the tessellattice returns them back to the particle, restoring its mass and speed.

But in our case, only a part of all the inertons of the hydrogen polaron, albeit a significant part, is absorbed by the lattice atom. This part of all the inertons has the total mass m_H^* (7) and hence the energy absorbed by the atom is $m_H^* c^2$, which varies from about 60 keV to 3 MeV.

This energy absorbed by the atom must be associated with its absorption of a mass defect, i.e. $\delta m \equiv m_H^*$ whose energy is $m_H^* c^2$. If the second term in the Hamiltonian (1) is related to this mass defect energy, then it becomes clear that such a high kinetic energy should complete contract the electron shells (whose total energy is usually less than 50 keV) and then also enters the nucleon of the atom under consideration, which puts also the nucleus in a contracted state (since nuclear forces are based on mass [25], the injection of a mass defect into the nucleus leads to a mass excitation of the nucleus).

The nucleon, absorbing the energy $m_H^* c^2$, goes into an excited state, i.e., it contracts, but then the nucleus emits a gamma quantum with the energy $h\nu \equiv m_H^* c^2$, and returns to the ground state.

This is a qualitative explanation of the newly discovered phenomenon – contraction of the nucleus caused by the effect of the absorbed mass defect.

One more possible reaction is associated with a direct nuclear transformation caused by a correspondently heavy mass defect δm . Namely, the squeezed electron shell of the nickel atom could get so close to the nucleus that the electrons would be able to tear a few protons from it, and indeed, this explains the observed appearance of Mn and Cr [3].

The disappearance of both gamma radiation and nuclear transmutation should occur only after significant damage to the crystal lattice, after which small hydrogen polarons could not be created.

Researchers who have studied low energy nuclear reactions and the appearance of extra heat from metal systems filled with a hydrogen/deuterium gas sometime measure weak neutron radiation. Such a phenomenon was studied and explained in our work [23], i.e., it was demonstrated that those were not real neutrons, but neutron imitators, namely subhydrogens.

4. ANOMALOUS HEAT EFFECT

As mentioned in Introduction, successful experiments in which anomalous heat was generated were performed on samples of nickel powder or nickel nanoparticles (with various additives such as palladium, copper, etc.). Small grains of nickel powder should also be close to nickel nanoparticles, in some aspects. Of course, in such metal systems the crystal lattice is not extended and a typical angular frequency of atom vibrations is $> 10^{12} \text{ s}^{-1}$, and hence the number of phonons is small $(e^{\hbar\Omega/(k_B T)} - 1)^{-1} \sim 1$, which means that the formation of a hydrogen polaron is impossible. Therefore, gamma radiation should not occur.

The researchers [14] claim that the phenomenon of heat generation caused by hydrogen happens rather on the surface of the nanoparticles. Storms [36] recently noted that samples in which heat excess is displayed (presumably due to possible low-energy nuclear reactions) manifest changes in the chemistry.

The experiments [37] studied the trapping and transport phenomena of hydrogen in nickel and they revealed that both hydrogen trapping at grain boundaries and short-circuit diffusion through grain boundaries in nickel are present. The hydrogen trap activation energy at dislocations is lower than the activation energy for the bulk diffusion of hydrogen. The trap binding energy at grain boundaries was estimated as $20.5 \text{ kJ}\cdot\text{mol}^{-1}$ ($= 3.404 \times 10^{-17} \text{ J} = 0.2125 \text{ eV}$).

Paper [38] indicates that there is still great uncertainty about the value of the surface energy of nanoparticles. The authors associate uncertainty with the reduced number of next neighbours of surface atoms with decreasing nanoparticle size. But what is most interesting for us, they state that the surface itself is characterised by a disordered or quasi-liquid layer, which also supports the balance of the reduction of the binding energy between the atoms with decreasing particle size. The surface energy is estimated at around $1 \text{ J}\cdot\text{mol}^{-1}$ ($1.66 \times 10^{-21} \text{ J} = 0.01 \text{ eV}$) for a particle with the size 5 to 10 nm, which is confirmed by other calculations [39]. The strain energy of a nanoparticle is two orders of magnitude lower [38].

Recently the researchers [40] have studied the hydrogen segregation energy spectrum at the grain boundaries of polycrystalline nickel theoretically by exploring all the topologically favourable segregation sites. Their approach has allowed them to calculate the equilibrium hydrogen concentrations at grain boundaries, which turned out to be two to three orders of magnitude higher than the concentration inside the grains. In addition, they have found that the calculated grain boundary diffusion coefficient is three orders of magnitude greater than that of lattice.

Thus, in nanoparticles and metal grains hydrogen atoms are able to accumulate in the near-surface region. In these systems, the concentration of hydrogen atoms can exceed their concentration in bulk metals. Moreover, all kinds of traps, dislocations and impurities may significantly contribute to the effect of hydrogen accumulation. The point is that hydrogen atoms can gather in clusters, but this requires the presence of at least two different subsystems [41, 25]. Electronegativity [42] for nickel is equal to 1.91 and the difference between the value of hydrogen electronegativity, which is equal to 2, and this value is 0.09. If the difference is lesser than 0.5, this means that nonpolar bonds should be organised in the metal when a hydrogen gas H fills it (a similar situation takes place in copper, iron and many other metals). In the case of a nickel powder or sandwich containing layers of nano-nickel filled with a hydrogen gas, a network of hydrogen clusters should form.

The formation of clusters in condensed matter follows from the Hamiltonian

$$H(n) = \sum_s E_s n_s - \frac{1}{2} \sum_{s,s'} V_{ss'}^{\text{attraction}} n_s n_{s'} + \frac{1}{2} \sum_{s,s'} V_{ss'}^{\text{repulsion}} n_s n_{s'} \quad (8)$$

and the further investigation of the statistic sum of a system of interacting particles

$$Z = \sum_{\{n\}} \exp[-H(n)/(k_B T)] \quad (9)$$

where E_s is the kinetic energy of a particle being in the s th state, the potentials $V_{ss'}$ represent the paired energy or attraction/repulsion between particles located in s and s' states, and the filling numbers n_s have only two meanings: 1 and 0 [43, 25].

A detailed consideration of this problem results in the derivation of a simple action, which for a classical system for one cluster looks as below

$$S_1 \approx a(N)N - 2b(N)N \quad (10)$$

where the functions

$$a(N) = \frac{3}{k_B T} \int_1^{N^{1/3}} V^{\text{repulsion}}(x) x^2 dx, \quad (11)$$

$$b(N) = \frac{3}{k_B T} \int_1^{N^{1/3}} V^{\text{attraction}}(x) x^2 dx \quad (12)$$

and N is the number of particles in the cluster.

A model system of N particles (atoms, molecules) interacting through the Lennard-Jones potential resulted in the solution [25, Sect. 5.4.2]

$$N = \left(\frac{5}{24} \frac{V_0}{m_H \omega^2 \delta r^2} \right)^{\frac{2}{5}} \quad (13)$$

where V_0 is the potential energy of interaction between two nearest atoms, or the interatomic potential for atom pair (in our case for two hydrogen atoms), m_H is the mass of hydrogen atom, ω is the angular frequency of hydrogen atoms oscillating in the cluster near their equilibrium positions and δr is the amplitude of these oscillations. The elastic energy $\frac{1}{2} m_H \omega^2 \delta r^2$ is treated as the submicroscopic potential that balances the system of particles in question, which interact through electrostatic interaction. Once again, it is the inerton interaction that ensures the creation of a cluster.

A typical size of nanoparticles used for the study of the anomalous heat effect varies from 5 to 10 nm. In the case of nickel, the concentration of its atoms is about $9 \cdot 10^{28} \text{ m}^{-3}$, which allow us to estimate the number of atoms in such nanoparticles: 47.124 and 5.890, respectively. The concentration of hydrogen atoms in nanoparticles are higher than in the bulk nickel, nevertheless, it has to be comparatively small in comparison with the number of nickel atoms. We can assume that the number of H atoms ranges from several hundred (for large nanoparticles) to several dozen (for small particles).

For example, we can put $V_0 \approx 4.5 \times 10^{-21} \text{ J}$ ($= 0.028 \text{ eV}$), $\omega \approx 10^{11} \text{ s}^{-1}$, and $\delta r \approx 2 \cdot 10^{-11} \text{ m}$. Substituting these parameters into expressions (11) and (12), we obtain the number of hydrogen atoms assembled in the cluster, $N \approx 150$. It is interesting to see that temperature effects drop out of the cluster formation equations. Nevertheless,

clusters are rather dynamic, that is, they are not too stable, and they can probably disintegrate and then quickly form again in the nanoparticle close to its inner surface, where atom hydrogens gather [40].

But how do hydrogen atoms diffuse within and between nanoparticles? They seem to diffuse both as individual atoms and as a whole cluster. The activation energy for these two different diffusing objects must be different. An individual H can be trapped by inhomogeneities and impurities and hence its activation energy should be comparatively high. On the other hand, the cluster as a whole can move with much less activation, since a certain kinetic energy is concentrated in its own oscillations, which causes it to overcome the opposite energy barrier. The speed of cluster movement is determined by its temperature T

$$\frac{1}{2}Nm_H v_{cl}^2 = \frac{3}{2}k_B T \quad (14)$$

where Nm_H is the mass of the cluster. Then the momentum for the moving cluster of hydrogen atoms should be written as follows

$$Nm_H v_{cl} = \sqrt{3Nm_H k_B T} e^{-E_{a, cl}/(k_B T)} \quad (15)$$

Here, the activation energy of the cluster energy is a fitting parameter, but it should be small because individual hydrogen atoms have a tendency to move similar to the movement of gas molecules. Let us put it equal to $E_{a, cl} = 3.45 \times 10^{-21}$ J ($= 0.022$ eV).

Let us now plot graphs for the momentum of a nickel atom (2), which oscillates around its equilibrium position in the lattice, and for the momentum of a cluster of hydrogen atoms (15) as a function of temperature. Fig. 2 illustrates the behaviour of these momenta versus temperature.

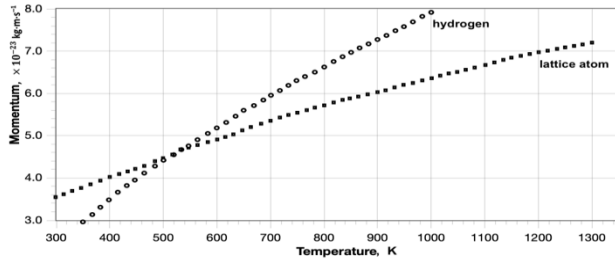


Fig. 2 – Momenta of an oscillating atom of the crystal lattice and a diffusing cluster of hydrogen atoms vs temperature T

As can be seen, the behaviour curves of the two momenta intersect about $T = 500$ K. This point of intersection means the momentum resonance. The curve for the momentum of the cluster is plotted using the parameters N and $E_{a, cl}$ specified above. However, this value can vary depending on the place in which the cluster is located in a nanoparticle and also can vary from nanoparticle to nanoparticle or from a grain to grain. Therefore, in general for the sample studied we can anticipate that the points of intersection of the two curves lie in a wide range of temperatures, from about 400 K to 1000 K.

What happens during a resonant collision? When an atom of the lattice collides with a cloud of hydrogen atoms that form a cluster, the inerton cloud of the atom jumps to the cluster, transferring the kinetic energy of the atom to it. The moment of collision is shown in Fig. 3.

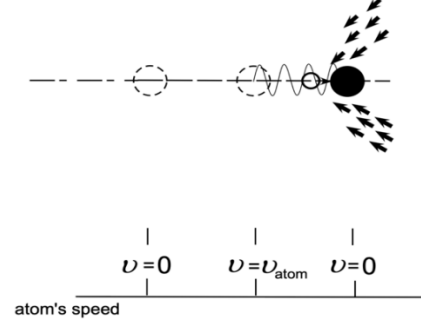


Fig. 3 – The atom collides with the hydrogen cluster, such that the atom's inerton cloud jumps from the atom to the cluster.

And now the climax happens. The system studied is in thermostat conditions, which is usually described as an infinite set of Bose oscillators

$$\sum_q \hbar \omega_q \left(\hat{b}_q^\dagger \hat{b}_q + \frac{1}{2} \right).$$

This thermostat is treated as a background that is always available and maintains the system studied in balance with the environment. Bose operators support the exchange of energy quanta between the system and the environment. So, if an atom loses its kinetic energy, the thermostat will restore its state (restores both the mass state and the atom's kinetic energy) in a time t_{relax} that can range from picoseconds to nanoseconds.

But the cluster in question is different. The cluster requires energy from inertons that are able to bind its hydrogen atoms. Hence, the formation of cluster, having taken over the momentum and inertons from the atom of the lattice (Fig. 3) can be considered as compression of the hydrogen gas. It is a matter of fact that compression of a gas leads to an increase in its pressure and temperature. Consequently, the subsequent scattering of the cluster on the lattice vibrations will lead to the transfer of heat to the lattice and the disintegration of the cluster into individual hydrogen atoms.

The kinetic energy that an atom of the lattice passes to the cluster (Fig. 3) can be easily estimated. Indeed, $v_{Ni} = \sqrt{3k_B T / m_{Ni}}|_{T=500 K} = 461 \text{ m}\cdot\text{s}^{-1}$, then the kinetic energy of the crystal atom $\frac{1}{2}m_{Ni}v_{Ni}^2 = 1.036 \times 10^{-20}$ J ($= 0.0646$ eV). Let us assume that all this energy, without dissipation, is converted into the energy of the cluster. Then one atom of H accounts for one 150th of this value: $\mathcal{E}_1 = 6.9 \times 10^{-22}$ J ($= 4.31 \times 10^{-4}$ eV), since above we assume that the number of H atoms in a cluster $N = 150$. Let Δt is the lifetime of the cluster after which the cluster energy is passed into the metal lattice of the system of nanocomposites studied. If we put $\Delta t = 10^{-3}$ s then the energy that can be transferred from the hydrogen subsystem to the metal nanoparticle per hydrogen atom

will be at most: $\mathcal{W}_1 = \mathcal{E}_1/\Delta t = 6.9 \times 10^{-19} \text{ W}$.

1 gram of nickel sample contains $9 \cdot 10^{22}$ atoms, so we may assume that such a sample can absorb at least $N_{\text{total}} = 9 \cdot 10^{17}$ atoms of hydrogen. Then, in total, all hydrogen atoms, which fill the nanocomposite metal system, will be able to generate $\mathcal{W} = N_{\text{total}}\mathcal{W}_1 \approx 6.2 \text{ W}$ of thermal power. This is a reasonable theoretical explanation of the phenomenon known as the anomalous heat effect.

Note in a certain sense, such a cluster in a nanoparticle resembles the mitochondrion organelle that lives in a living cell proving the cell with energy.

5. CONCLUDING REMARKS

Thus, the main reason leading to the appearance of gamma radiation in the composite metal samples in question has been related to the formation of a hydrogen small polaron, whose diffusion is activated by crystal lattice vibrations. The radiation effect itself is due to the resonant collision of the polaron with the opposite atom of the lattice. During momentum resonance, the hydrogen atom transfers its inerton cloud to the lattice atom. This leads to an elastic mass excitation of the electron shell of the atom, and then the mass excitation penetrates into the nucleus, leading to squeezing of the nucleons. Of course, the nucleus eliminates such excitation by emitting a gamma ray whose energy corresponds to the absorbed elastic energy of the inerton cloud of the hydrogen atom.

Essentially, this is the method the sample uses to remove excess heat. In fact, the emission of gamma quanta causes cooling of the system, but the system is open, i.e., it is in a thermostat that constantly maintains its thermodynamic equilibrium. Also, various authors indicated that they registered slow neutrons of insignificant intensity, but a detailed study of these neutrons proves that they are actually hydrogen subatoms [23, 24]: a proton captures a free electron in the presence of the inerton cloud of the crystal atom, which reduces the size of the hydrogen atom by three orders of magnitude, bringing it closer to the size of the atomic nucleus; because of this, such an entity was called subhydrogen.

A subhydrogen is a main carrier that triggers a number of nuclear transmutations and is also responsible for the proton-proton chain of nuclear reactions [43].

The outward emission of energy by a quantum physical system is a common occurrence, although the inclusion of knowledge on the submicroscopic concept of physics is necessary for understanding the phenomenon. However, the radiation of the system into itself looks somewhat unusual and that is why researchers called this phenomenon an anomalous thermal effect.

Nevertheless, there is nothing unusual about this phenomenon. But in order to understand the mechanism, it is necessary to apply the knowledge of submicroscopic physics, which allows studying physical phenomena at a level of detail that is unacceptable and impossible in

quantum mechanics.

In principle, the generation of heat inside the nanocomposite metal system is analogous to a heat pump: air – water, water – water, earth – water, etc. The only difference is that it is necessary to change the style of thinking from classical mechanics and thermodynamics to submicroscopic mechanics.

At a microscopic level, a gas of hydrogen atoms acts as the refrigerant in a heat pump shown in Fig. 4. Due to the absorption of inertons coming from the metal subsystem, gaseous hydrogen is compressed (stages 2 and 3) into a cluster (stage 4). In the cluster state, the kinetic energy of the hydrogen subsystem increases significantly, and then it is released (stage 1) upon collision with metal atoms of the nanosystem and thus heats the entire system under study. After the scattering, the cluster disintegrates into free hydrogen atoms, and so on...

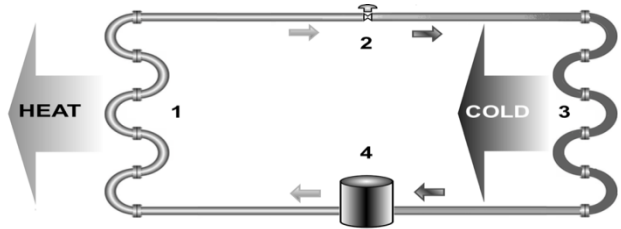


Fig. 4 – A mechanical heat pump uses the physical properties of a volatile liquid that evaporates and condenses, known as a refrigerant. The heat pump compresses the refrigerant to make it hotter on the side that heats up and depressurises it on the side where heat is absorbed. The pump's vapor-compression refrigeration cycle: 1) condenser, 2) expansion valve, 3) evaporator, 4) compressor

There is another potential possibility, which is that a nickel atom, at the moment of collision in the presence of a free electron, throws its inerton cloud or part of it onto a single hydrogen atom. Then the formation of a hydrogen ion, H^+ , is possible, and this ion will have relatively significant kinetic energy, which it will gradually dissipate in the system under study. The presence of negative hydrogen ions has long been known (see e.g. [44-50]). However, to implement such a possibility, a resonant collision by momentum is required between a metal atom and independent hydrogen. But the kinetic parameters of these two entities do not bring them to a direct resonance by momentum. Therefore, such a mechanism should be considered as acceptable, but still secondary (although it is interesting to investigate whether inertons are involved in the binding of a free electron to a hydrogen atom or molecule).

Finally, anomalous heat release is caused by the transition of free hydrogen atoms to the cluster state with their subsequent scattering by lattice vibrations, which occurs in the style of a heat pump.

REFERENCES

1. T. Ohmori, M. Enyo, *Fusion Technology* **24** No 3, 293 (1993).
2. S. Focardi, V. Gabbani, V. Montalbano, F. Piantelli, S. Veronesi, *Nuovo Cimento A* **111**, 1233 (1998).
3. E.G. Campari, S. Focardi, V. Gabbani, V. Montalbano, F. Piantelli, E. Porcu, E. Tosti, S. Veronesi, *Proc. of the 8th Int. Conf. on Cold Fusion: Lerici (La Spezia)* (Ed. by F. Scaramuzzi, Italian Physical Society, Bologna, 2001), 69 (Italy, 21-26 May 2000).
4. S. Focardi, V. Gabbani, V. Montalbano, F. Piantelli, S. Veronesi (*Marseille: France: 2004*);
5. E. Campari, G. Fasano, S. Focardi, G. Lorusso, V. Gabbani, V. Montalbano, F. Piantelli, C. Stanghini, S. Veronesi, *Condensed Matter Nuclear Science*, 405 (Ed. by J. P. Biberian) (World Scientific Publishing: Singapore: 2006).
6. A. Rossi, *Method and Apparatus for Carrying Out Nickel and Hydrogen Exothermic Reactions*, Patent application WO 2009125444, published 2009-10-15.
7. G. Levi, E. Foschi, T. Hartman, B. Höistad, R. Pettersson, L. Tegnér, H. Essén, *arXiv* (2013).
8. G. Levi, E. Foschi, B. Höistad, H. Essén, *Observation of Abundant Heat Production from a Reactor Device and of Isotopic Changes in the Fuel* (2014).
9. A.G. Parkhomov, S.N. Zabavin, T.R. Timerbulatov, K.A. Alabin, S.N. Andreev, A.G. Sobolev, *Nuclear Phys.* **9** No 1, 74 (2018).
10. T. Clarke, *Comment on the Report "Observation of Abundant Heat Production from a Reactor Device and of Isotopic Changes in the Fuel"* (2015)
11. E.J. Beiting, *Aerospace Report No. ATR-2017-01760* (2017).
12. N.M. Evstigneev, A.V. Ikonnikov, S.V. Makeev, O.I. Ryabkov, V.V. Skliznev, *J. Phys. Commun.* **5** No 10, 105021 (2021).
13. F. Celani, E.F. Marano, A. Spallone, *J. Condens. Matter Nucl. Sci.* **13**, 56 (2014)
14. A. Takahashi, A. Kitamura, R. Seto, Y. Fujita, T. Y. Furuyama, T. Murota, T. Tahara, *J. Condens. Matter Nucl. Sci.* **15**, 1 (2014).
15. G.K. Hubler, K.K. Katti, D. Pease, A.E. Boher, O. Azzizi, J. He, K.V. Katti, *J. Condens. Matter Nucl. Sci.* **36**, 38 (2022).
16. A. Kitamura, A. Takahashi, K. Takahashi, R. Seto, T. Hatano, Y. Iwamura, T. Itoh, J. Kasagi, M. Nakamura, M. Uchimura, H. Takahashi, S. Sumitomo, T. Hioki, T. Motohiro, Y. Furuyama, M. Kishida, H. Matsune, *Int. J. Hydrogen Energy* **43**, 16187 (2018).
17. Y. Iwamura, T. Itoh, J. Kasagi, A. Kitamura, A. Takahashi, K. Takahashi, R. Seto, M. Uchimura, H. Takahashi, T. Hioki, T. Motohiro, Y. Furuyama, M. Kishida, H. Matsune, *J. Condens. Matter Nucl. Sci.* **29**, 119 (2019).
18. A. Takahashi, T. Yokose, Y. Mori, A. Taniike, Y. Furuyama, H. Ido, A. Hattori, R. Seto, A. Kamei, J. Hachisuka, *J. Condens. Matter Nucl. Sci.* **33**, 14 (2020).
19. A. Takahashi, T. Yokose, Y. Mori, A. Taniike, Y. Furuyama, H. Ido, A. Hattori, R. Seto, A. Kamei, J. Hachisuka, *Proc. JCF* **20**, 9 (2020).
20. Y. Iwamura, J. Kasagi, T. Itoh, T. Takahashi, M. Saito, Y. Shibasaki, S. Murakami, *J. Condens. Matter Nucl. Sci.* **36**, 285 (2022).
21. Y. Iwamura, T. Itoh, S. Yamauchi, T. Takahashi, *Jpn. J. Appl. Phys.* **63**, 037001 (2024).
22. T. Mizuno, J. Rothwell, *Preprint; in The 22nd International Conference for Condensed Matter Nuclear Science ICCF-22, Assisi, Italy* (2019).
23. V. Krasnoholovets, Yu. Zabulonov, I. Zolkin, *Univer. J. Phys. Appl.* **10** No 3, 90 (2016).
24. V. Krasnoholovets, *J. Advanced Phys.* **5**, 168 (2016).
25. V. Krasnoholovets, *Structure of Space and the Submicroscopic Deterministic Concept of Physics* (Apple Academic Press: CRC Press: Toronto-New York-New Delhi: 2017).
26. Y. Fukai, *The Metal-Hydrogen System. Basic Bulk Properties* (Springer: Berlin-Heidelberg: Germany: 2005).
27. R. Hempelmann, *J. Less-Common Metals* **101**, 69 (1984).
28. A. Braun, Q. Chen, *Nat. Commun.* **8**, 15830 (2017).
29. R. Martínez-Casado, J.L. Vega, A.S. Sanz, S. Miret-Artés, *J. Chem. Phys.* **126** No 19, 194711 (2007).
30. C.T. Chudley, R.J. Elliott, *Proc. Phys. Society* **77** No 2, 353 (1961).
31. V.V. Krasnoholovets, P.M. Tomchuk, S.P. Lukyanets, *Advances in Chemical Physics*, **125**, 351 (Eds. by V. Prigogine, S.A. Rice) (John Wiley & Sons, Inc.: 2003).
32. M. Velasco-Plascencia, O. Vázquez-Gómez, L. Olmos, F. Reyes-Calderón, H.J. Vergara-Hernández, J.C. Villalobos, *Catalysts* **13** No 3, 517 (2023).
33. D.O. Hayward, P.J. Herley, F.C. Tompkins, *Surf. Sci.* **2**, 156 (1964).
34. Y.-S. Chen, C. Huang, P.-Y. Liu, H.-W. Yen, R. Niu, P. Burr, K.L. Moore, E. Martínez-Pañeda, A. Atrens, J.M. Cairney, *Int. J. Hydrogen Energy* **136**, 789 (2024).
35. A. Metsue, A. Oudriss, X. Feaugas, *MRS Adv.* **1**, 1785 (2016).
36. E. Storms, *Preprint* 6/1/23 (2023)
37. S.-M. Lee, J.-Y. Lee, *Metallurg. Trans. A* **17**, 181 (1986).
38. D. Vollath, F.D. Fischer, D. Holec, *Beilstein J. Nanotechnol.* **9**, 2265 (2018).
39. X.H. Yu, J. Rong, T.L. Fu, Z.L. Zhan, Z. Liu, J.X. Liu, *J. Computat. Theor. Nanosci.* **12**, 1 (2015).
40. Y. Ding, H. Yu, M. Lin, M. Ortiz, S. Xiao, J. He, Z. Zhang, *J. Mater. Sci. Technol.* **173**, 225 (2024).
41. V. Krasnoholovets, B. Lev, *Cond. Matter Phys.* **6** No 1, 67 (2003).
42. *Pauling Electronegativity*, Wikipedia
43. V. Krasnoholovets, *Mechanisms of Low Energy Nuclear Reactions and the Mechanism of Nuclear Fusion in the Sun* (In Press).
44. J. Hiskes, *J. Phys. Colloques* **40** No C7, 179 (1979).
45. A.R.P. Rau, *J. Astrophys. Astr.* **17**, 113 (1996).
46. Z. Juhász, B. Sulik, J. Rangama, E. Bene, B. Sorgunlu-Frankland, F. Frémont, J.-Y. Chesnel, *Phys. Rev. A* **87**, 032718 (2013).
47. V.P. Goretskii, A.M. Dobrovolskiy, *Probl. At. Sci. Technol.* **98** No 4, 315 (2015).
48. S. Roy, C. Sinha, *arXiv* (2008).
49. B.K. Gupta, *Physica* **25**, No 1-6, 190 (1959).
50. B. Jordon-Thaden, H. Kreckel, R. Golser, D. Schwalm, M.H. Berg, H. Buhr, H. Gnaser, M. Grieser, O. Heber, M. Lange, O. Novotny, S. Novotny, Henrik B. Pedersen, A. Pettrignani, R. Repnow, H. Rubinstein, D. Shafir, A. Wolf, D. Zajfman, *Phys. Rev. Lett.* **107**, 193003 (2011).

Механізм виділення тепла з нікелю або іншого металу, наповненого воднем**В. Красноголовець***Інститут фізики, НАНУ, 03028 Київ, Україна*

Показано, що поява гамма-випромінювання в композитних металах, наповнених воднем, відбувається в результаті імпульсного резонансу між розсіяним воднем, що дифундує в поляронному режимі, та атомом кристалічної решітки, який неперервно осцилює. Причина генерації додаткового тепла в металевих нанокompозитах та зернах полягає в розсіюванні коливального атома кристалічної решітки на атомах водню, в результаті чого утворюється кластер водню, який відбирає кінетичну енергію від атома. Навколишній термостат швидко повертає атом до теплової рівноваги, і лише після цього кластер віддає захоплену енергію назад атому решітки, що збільшує кінетичну енергію атома, тобто призводить до збільшення нагрівання зразка, а сам кластер знову розвалюється на вільні атоми. Далі така процедура повторюється знову і знову. Таким чином, виявлено нову особливість нанокompозитних матеріалів, а саме можливість короткочасного накопичення енергії.

Ключові слова: Тепло, Водень, Інертони, Дефект маси, Наночастинки.